

Synthesis of N-doped Graphene for Simultaneous Electrochemical Detection of Lead and Copper in Water

Caihong Lei¹, Shenghua Zhang^{2,*}, Suping Zhao¹

¹ Hangzhou Polytechnic, Hangzhou, Zhejiang, 311402, P.R. China

² Institute of Urban Environment, Chinese Academy of Science, Fujian Xiamen, 361021, P.R. China

*E-mail: zhangshenghua5@yeah.net

Received: 11 January 2017 / Accepted: 22 March 2017 / Published: 12 May 2017

In the study, glassy carbon electrode (GCE) modified by nitrogen doped graphene (N-GE) is employed to simultaneously determine copper & lead in an electrochemical approach that features favorable sensitivity and speed. In comparison to original GCE, GCE modified by N-GE exhibited remarkably boosted electrochemical activity as for square wave anodic stripping voltammetry. The detection range of copper exhibited in reduced graphene oxide (RGO) modified GCE was wide from 0.05 to 2.5 μM , with a detection limit of 11 nM, while that of lead was from 0.05 to 2.5 μM with a detection limit of 5 nM. Besides, the proposed sensor was significantly reproducible with a desirable performance in anti-interference.

Keywords: Graphene; Doping; Electroanalysis; Heavy metal ions; Lead; Copper

1. INTRODUCTION

Being seriously hazardous to environment & human health and unable to be biodegraded, the contamination of heavy metal has been a prominent issue. In order to detect toxic metals rapidly, specific ion sensors development has been explored by numbers of researchers [1, 2]. In diverse fields like casting, mining and manufacturing, the outstanding heavy metals of copper and lead have gained wide exploitation and discharging [3]. To be more detailed, Pb^{2+} contamination with toxicity has been led to during the extensive adoption of lead throughout the history of humankind [4]. Excessive lead intake would cause the brain and other organs to malfunction, as well as impede the development of fetus. Meanwhile it is related to diseases concerning kidney, neurology, haematology and neurology [5, 6]. Furnace atomic absorption spectroscopy & polarography approach constitute two analytical ways of detecting lead. Both of them entail long period and cost much, despite their sensitivity for

detecting lead [7]. Meanwhile, diverse intoxications could be brought through excessive copper intake. For instance, the pathogenesis about diseases such as Parkinson's disease, Alzheimer's disease, Wilson's disease, Menkes syndrome and amyotrophic lateral sclerosis would be caused by imbalanced cellular processes. Note that the imbalanced process results from the increased copper cations concentration in body [8-12]. Atomic adsorption spectrometry, colorimetric analysis, inductively coupled plasma-mass spectrometry, ion chromatography etc. have been adopted to detect copper ions [13-20]. Nevertheless, a majority of them require plenty of time and money and include complex operation procedures.

Thus electrochemical sensor is another effective method to detect copper and lead in that it can be rapidly applied on-site, conveniently operated, and is favorable as for the costs of instruments [21]. The electrode modification is achieved via numbers of materials to improve its electrochemical behavior. Carbon modifier could have the electrode improved in electrochemical behavior, as revealed by a great deal of researches [22, 23]. Featuring special chemical and physical traits, graphene has been appealing to researchers in many fields as for experiments and theories since its discovery in 2004 [24]. The traits include high surface areas, high mechanical property, excellent electronic transport property, etc. This material is promisingly likely to be applied in various forms including battery, catalyst, supercapacitors, sensors, etc. due to its merits above [25-27]. The electronic traits of host materials can be modified through a desirable method, chemical doping with hetero-atoms. The chemical reactivity and electronic traits would go through great changes caused by graphene doped with hetero-atoms, which could also bring the disruption of carbon atoms' ideal sp^2 hybridization [28]. The formation of strong valence bonds could be achieved through the cooperation of carbon atoms and nitrogen that possesses five valence electrons and similar atomic size. Herein, located near carbon in period table, nitrogen is considered fantastic for doping [29]. The modulation of the band structure of graphene would be achieved with the replacement of carbon atoms into the graphene frameworks, where its excellent performance in conductivity is not affected [30]. Currently, there are diverse approaches to fabricating nitrogen-doped graphene (N-GE), including chemical vapor deposition with NH_3 gas [31], nitrogen plasma treatment of graphene, thermal annealing graphite oxide with melamine [32], high-power electrical annealing in NH_3 [33], hydrothermal approach with $NH_3 \cdot H_2O$ or urea as the nitrogen precursor [34, 35], etc. Favourable electrocatalytic activity of N-GE materials synthesized through diverse ways is shown to various molecules. Note that 'pyrrolic' N and/or 'pyridinic' N function as the main reason for such activity, according to these literatures.

This study explored the fabrication of an electrochemical sensor on the basis of N-doped graphene modified electrode, in order to determine copper and lead simultaneously. The modified electrode has its behaviour evaluated via square wave anodic stripping voltammetry (SWASV). It also demonstrated the reproducibility and anti-interference trait of the fabricated sensor.

2. EXPERIMENTS

2.1. Materials

Graphite powder was commercially available in Shanghai Carbon Co., Ltd. Boron trifluoride diethyl etherate purchased from BFEE, Sinopharm Chemical Reagent Co., Ltd. went through

distillation-purification through before adoption. Being of analytical grade, all other adopted reagents went through no further purification. Besides, Milli-Q water was adopted through all the experiments.

2.2. Preparation of nitrogen-doped graphene

Graphite oxide (GO) was first prepared from natural graphite powder by a designed approach [36]. With the raw material of GO, N-GE was generated through doping and reduction by urea via wet-chemical approach [37]. In general, with a concentration of 0.5 mg/mL, the exfoliated GO solution (150 mL) was infused into with a three-necked flask. The pH of 8.0 was achieved for GO dispersion through the modulation of diluted ammonia solution, followed by the addition of 5.0 g of urea through powerful stirring. After the temperature elevated to 95 °C, the solution went through 30 h of reflux. Subsequently, coagulation was caused through the addition of the diluted HCl to as-prepared N-GE dispersion. Then repeated centrifugation was conducted by double-distilled water and anhydrous alcohol to the resultant mixture. Eventually, the solid N-GE specimen was generated through vacuum drying. And the synthesis of RGO was conducted based on literatures to make comparisons [38]. X-ray photoelectron spectroscopy (XPS) measurements were performed on a scanning X-ray microprobe PHI Quantera II (Ulvac-PHI, INC.) with a C60 gun.

2.3. Electrode fabrication

Aluminum oxide slurries (0.3 and 0.05 μm) were adopted for the polishing of the original electrode. To remove the physically adsorbed substance, the modified electrode then went through 10 m double distilled water & ethanol cleaning in an ultrasonic way. Subsequently the ultrasonic dispersion of as-generated N-GE of certain volume into *N,N*-dimethylformamide (DMF) contributed to N-GE suspension (0.25 mg/mL), which was later dropped on the original GCE surface for later air evaporation of the solvent. Then the resultant electrode, N-GE/GCE, was eventually produced.

2.4. Electrochemical determination

Featuring a single-compartment cell with a traditional three-electrode, a CHI660D electrochemical workstation of CH Instrumental Co. in China was adopted for all electrochemical experiments. The working electrode, reference electrode and auxiliary electrode are respectively original or modified GCE, saturated calomel electrode (SCE) and a platinum wire. All potential values reported were given versus this reference electrode, if not differently stated. CV was conducted in PBS with 5 mM $[\text{Fe}(\text{CN})_6]^{3-/4-}$ using three conventional electrode with 50 mV/s scan rate. The EIS responses of the aptasensor were collected in 0.1 M PBS with a pH of 7.4 in the presence of 5 mM $[\text{Fe}(\text{CN})_6]^{3-/4-}$ couple (1:1). The anodic stripping of electrodeposited Hg(0) was performed from -0.5 to 0.5 V under optimized conditions (frequency, amplitude, potential increment were 40 Hz, , 20 mV, and 4 mV, respectively). For comparison purpose, a Perkin Elmer A Analyst 700 (Norwalk, CT, USA) atomic absorption spectrometer with deuterium background corrector was utilized for the study. Perkin

Elmer single element hollow cathode (HC) lamps were used for flame atomic absorption spectrometric determinations. All readings were taken using air/acetylene flame.

3. RESULTS AND DISCUSSION

With CV and EIS (Figure 1), this work explored the electrochemical performance of RGO/GCE, N-GE/GCE and original GCE in $[\text{Fe}(\text{CN})_6]^{3-/4-}$ solution (5.0 mM). Reversible redox peaks of $[\text{Fe}(\text{CN})_6]^{3-/4-}$ are shown for in all the CV curves (Figure 1). Nevertheless, redox peaks for N-GE/GCE excel those of RGO/GCE and original GCE in peak currents, and are the most reversible. The electrode designed by N-GE with great electrochemical trait performed better in electron shift than RGO/GCE and original GCE, as suggested in the above result. Besides, the poor performance in conductivity of RGO caused by its structure deficiencies resulted in less CV response at RGO/GCE compared with that at the original GCE.

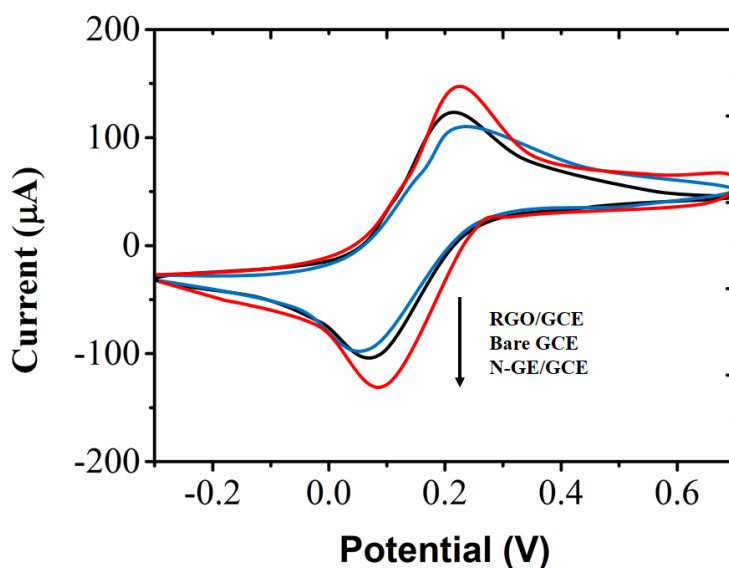


Figure 1. CVs of N-GE/GCE, original GCE and RGO/GCE in KCl solution (0.1 M) containing $[\text{Fe}(\text{CN})_6]^{3-/4-}$ solution (5.0 mM).

The sensor fabrication process is explored via EIS. A straight line at lower frequency range and a semicircle at higher frequencies make up an ideal impedance spectrum. Herein the former one strongly suggests a diffusion limit stage, and the electron-shift kinetics of the redox probe at the electrode interface is indicated by the diameter of the latter one. The marker ions, $[\text{Fe}(\text{CN})_6]^{3-/4-}$ solution (5.0 mM) containing KCl solution (0.1 M), were employed for the analysis of original GCE, RGO/GCE and N-GE/GCE at EIS frequency (0.1-10⁶ Hz), with their Nyquist plots revealed in Figure 2. The electron-transfer resistance of N-GE/GCE, GCE and RGO/GCE increased successively, with the successive impedance increase of them (Figure 2). N-GE performed excellently in electron

shift over the modified electrode surface, as indicated by the comparatively small semicircle diameter of the N-GE modified GCE. These results could be attributed to the increased conductivity of the nitrogen-doped graphene [39]. Moreover, the successful immobilization of N-GE on GCE was suggested by the impedance alterations of the modified electrode.

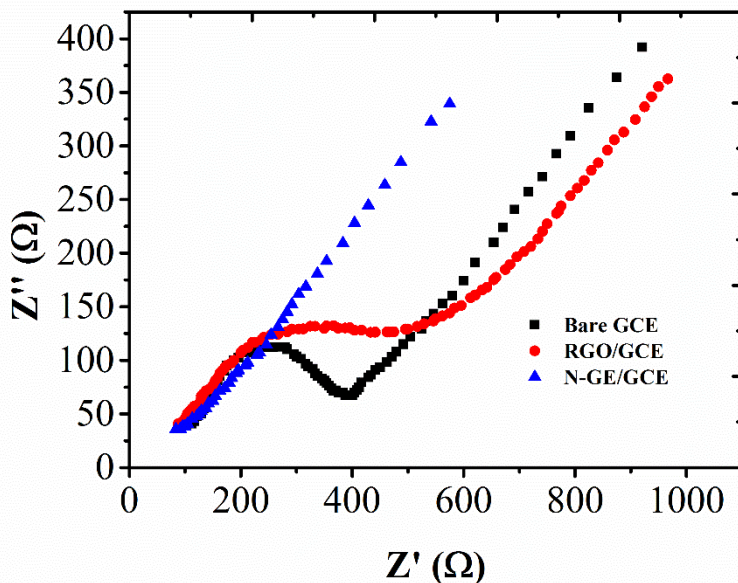


Figure 2. Nyquist plots of impedance spectra of the N-GE/GCE, original GCE and RGO/GCE in KCl solution (0.1 M) containing $[\text{Fe}(\text{CN})_6]^{3-/4-}$ solution (5.0 mM).

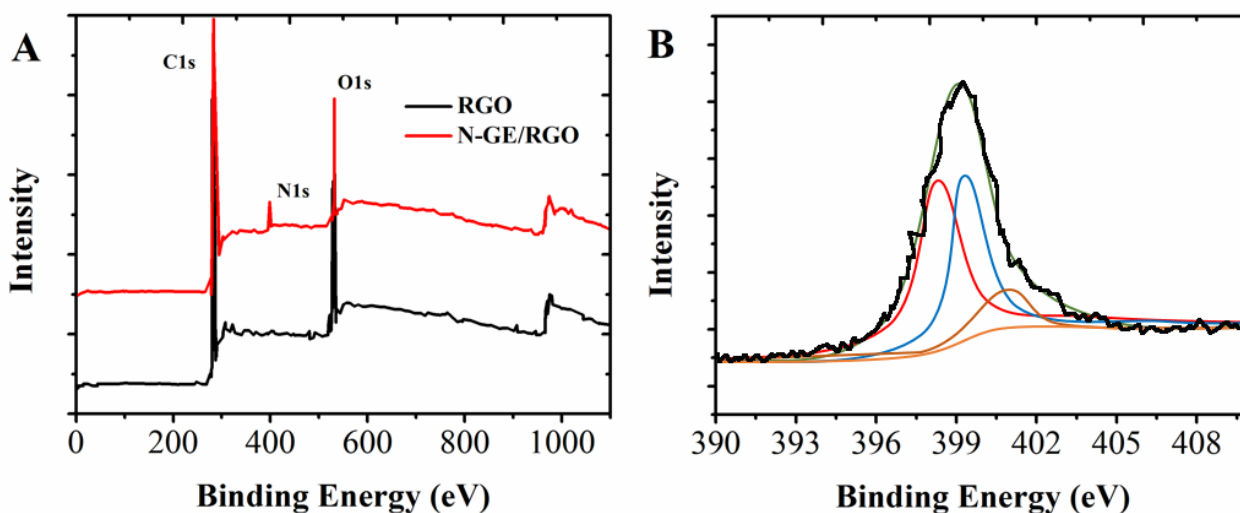


Figure 3. (A) XPS spectra of the RGO and the N-GE. (B) XPS N1s spectrum of the N-GE.

The XPS statistics in Figure 3 indicated that graphene was successfully doped with N. An O1s peak can be observed at ca.532 eV, while an obvious graphitic C1s peak appears at ca. 284.4 eV, as shown in the survey scan spectrum of RGO (Figure 3A). RGO spectrum exhibits no significant N peak, while that of N-GE shows a predominant N peak at ca. 400 eV, with 6.5% N in urea-reduced N-GE. Herein it can be verified that N atoms has been successfully incorporated to the graphitic layer of

graphene. N1s spectra in N-GE exhibits high-resolution, as indicated in Figure 3B. The ‘graphitic’ N, ‘pyrrolic’ N and ‘pyridinic’ N are respectively suggested through three predominant peaks of 402.2, 399.8 and 398.7 eV for binding energy. Notably, the amount of nitrogen incorporated in N-G was found to be approximately 15% with a high doping level. According to previous studies, the pyridinic nitrogen at graphene can provide a pair of electrons for conjugation with the π -conjugated rings which can introduce electron donor properties to graphene sheets and improve the electrochemical performances of N-G; the pyrrolic nitrogen has higher charge mobility in graphene due to better electron-donor characteristics and enhanced carbon catalytic activity in electron-transfer reactions [40]. The doping of graphene lattice with N atoms instead of carbon atoms suggests the formation of ‘graphitic’ N. It is likely for the p-electrons of ‘pyrrolic’ N and ‘pyridinic’ N to function in the form of π -conjugated system in the graphene. It can be suggested that a majority of N atoms are present in the form of ‘pyrrolic’ N and ‘pyridinic’ N, since through the comparison with the peaks for ‘graphitic’ N, those for ‘pyrrolic’ N and ‘pyridinic’ N occur more frequently (Figure 3B).

Subsequently, to determine Cu(II) and Pb(II) in the water, the work employed as-fabricated N-GE/GCE. In acetate buffer (0.1 M, pH 5.0) containing Cu(II) and Pb(II) (0.5 μ M) N-GE/GCE, RGO/GCE and original GCE have their analytical features demonstrated via SWASV in Figure 4. With the potential ranging from -0.5 to 0.5 V, two rather unobvious peaks can be monitored for the original GCE. 0.11 V and -0.22 are observed respectively as the typical stripping potentials for Cu(II) and Pb(II). The effective enhancement of electrode in its electrochemical behaviour was achieved as the surface of the carbon materials were modified, which was revealed through the comparatively higher peak currents at RGO/ITO. Besides, N-GE excels other counterparts in its electrocatalysis towards Cu(II) and Pb(II), as confirmed by much elevated and more vigorous peak currents at N-GE/GCE.

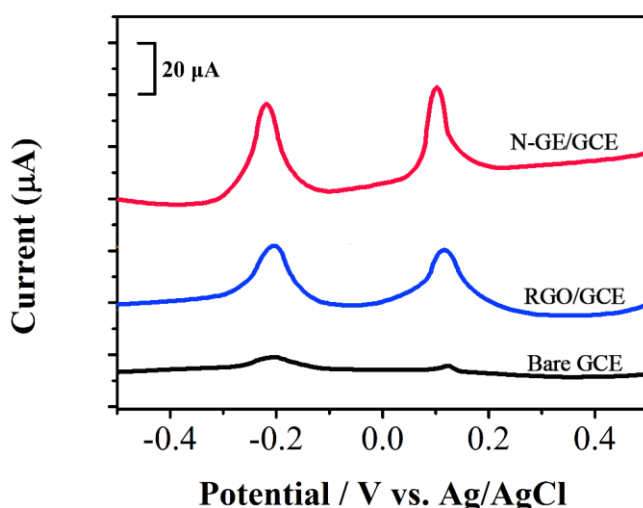


Figure 4. SWASVs for Cu(II) and Pb(II) (0.5 μ M) on original GCE, RGO/GCE and N-GE/GCE in acetate buffer (0.1 M, pH 5.0).

The significant enhancement of the electrode in its electrochemical behaviour was achieved through investigating the effect of the accumulation stage in this work. The influence of accumulation period and potential in the process of detecting Cu(II) and Pb(II) is indicated in Figure 5. -0.90 V was observed as the maximum current responses for Cu(II) and Pb(II) (Figure 3A). As the accumulation period increased from 0 to 150 s, a gradual rise for current responses could be observed, and no obvious alteration could be monitored with the extended accumulation time period (Figure 3B). Thus Cu(II) and Pb(II) determination opts for 150 s and -0.90 V accumulation herein.

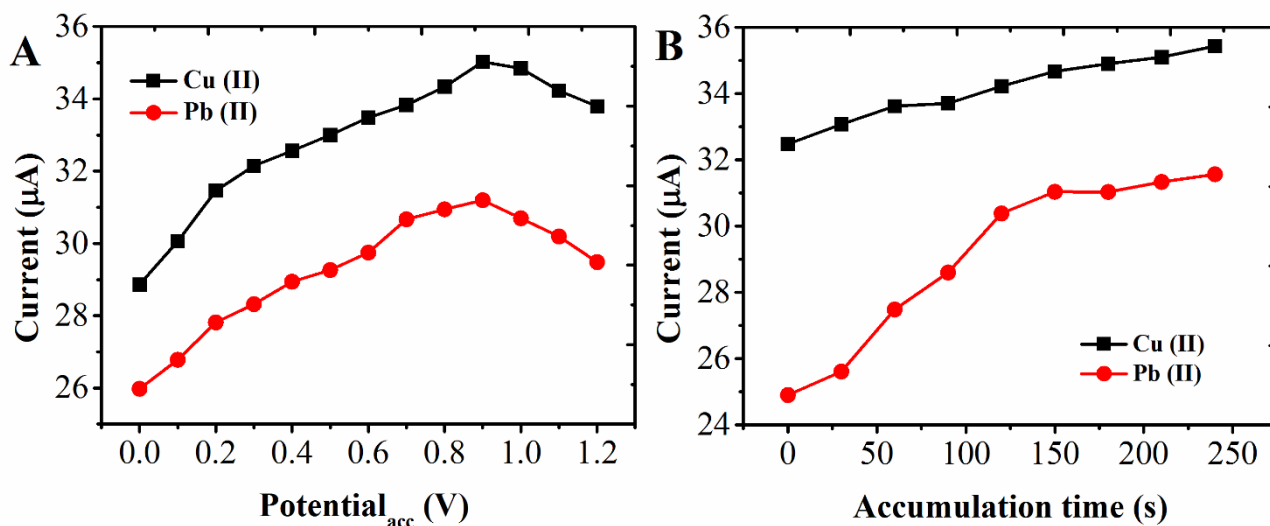


Figure 5. Effect of the (A) accumulation potential and (B) accumulation time period on the current response of Cu(II) and Pb(II) ($0.5 \mu\text{M}$) at N-GE/GCE.

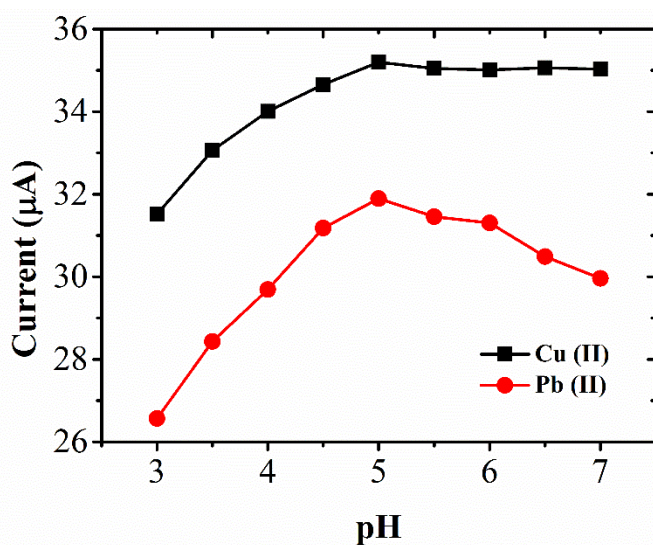


Figure 6. Effect of the pH values on the current response of Cu(II) and Pb(II) ($0.5 \mu\text{M}$) at N-GE/GCE.

This work also explored the influence of pH value in the process of electrochemically determining Cu(II) and Pb(II). As for the detecting process for Cu(II) and Pb(II), the pH value was

observed to be 3 to 7, whose influence was indicated in Figure 6. With the increase of pH from 3.0 to 5.0, the peak current for Cu(II) was observed to rise, and with the pH of 7.0 being obtained, it exhibited a similar response. Meanwhile, with the pH rising from 3.0 to 5.0, an increase of the peak current for Pb(II) was observed, followed by a drop as the pH increased to 7.0. Thus this work opted for pH 6.0 to determine Cu(II) and Pb(II).

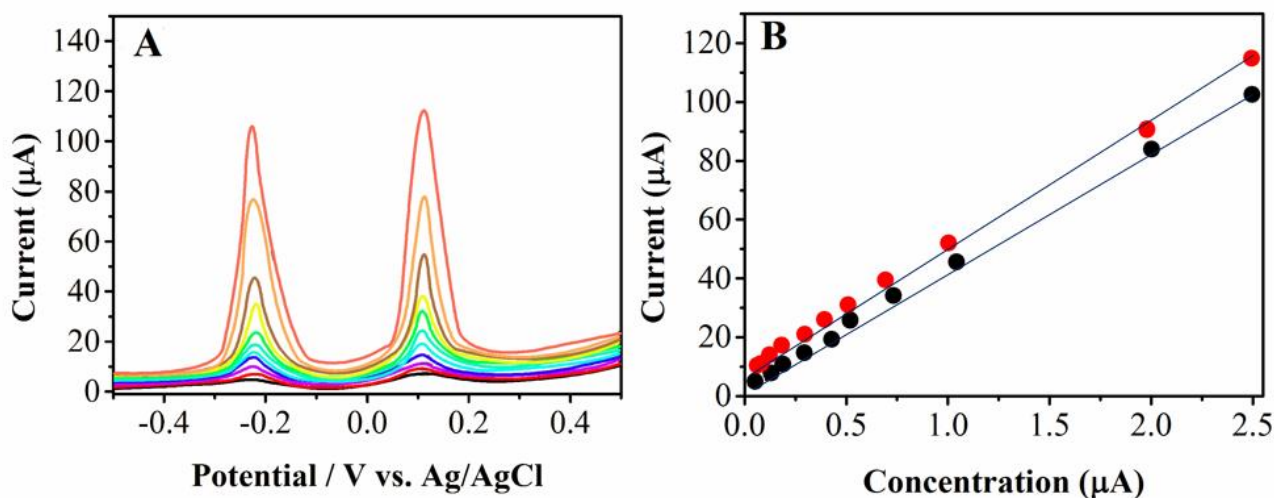


Figure 7. (A): SWASV response of the N-GE/GCE for the simultaneously analyzing Cu(II) and Pb(II) over a concentration range of 0.05 to 2.5 μM . (B) Plots of the value of anodic peak currents as a function of the concentration of Cu(II) and Pb(II).

Table 1. Detection limits (DL) and linear ranges (LR) of different modified electrodes for determination of Pb(II) and Cu(II).

Electrode	DL (Pb; Cu) μM	LR (Pb; Cu) μM	Reference
PolyL: poly(4-azulen-1-yl-2,6-bis(2-thienyl)pyridine)/GCE	0.014; —	0.1-20; —	[41]
BTSBA/GPE	0.062; 0.32	—; —	[42]
Bi/Au-GN-Cys/GCE	0.05; —	0.1-10; —	[43]
RGO/Bi/CPE	0.0055; 0.16	0.01-5; 0.2-20	[44]
$\text{Mo}_6\text{S}_x\text{I}_{9-x}$ NWS/GCE	0.045; 0.02	0.2-10; 0.5-5	[45]
N-GE/GCE	0.005; 0.011	0.02-2.5; 0.05-2.5	This work

Cu(II) and Pb(II) of diverse concentrations at N-GE modified GCE is characterized via SWASV curves in best experimental conditions in Figure 7. The range of 0.05 to 2.5 μM could be seen for the well-defined peaks, corresponding to the concentration of Cu(II) and Pb(II), with the linear regression equation of Cu(II) presented as $I_{\text{pa}} (\mu\text{A}) = 41.4348 c (\mu\text{M}) + 8.5031$, where the correlation coefficient is 0.978. On the other hand, the linear regression equation of Pb(II) can be presented as $I_{\text{pa}} (\mu\text{A}) = 37.8667 c (\mu\text{M}) + 5.2365$, where the correlation coefficient was 0.994. On the basis of signal-to-noise ratio of 3, Cu(II) could be detected as low as 5 nM, and Pb(II) as 11 nM through estimation.

Also, we have compared this electrode with some other different modified electrodes for the simultaneous determination of Pb(II) and Cu(II), as summarized in Table 1.

The developed protocol was applied for monitoring Pb²⁺ and Cu²⁺ ions in environmental and industrial effluents. In the industrial effluent about 0.5 μM of Pb²⁺ and in the lake water about 1.5 μM of Cu²⁺ were detected. Then this sample was spiked with a known amount of above said metal ions and analysed. The recoveries were found to be more than 95%. The results obtained with the proposed method were validated by the AAS method (Table 2).

Table 2. Determination of Pb²⁺ and Cu²⁺ in environmental and industrial effluents (*n* = 3)

	N-GE/GCE (μM)	AAS (μM)	Added (μM)	N-GE/GCE (μM)	AAS (μM)	Recovery (%)N-GE/GCE	RSD (%)	Recovery (%) AAS
Sample 1								
Pb ²⁺	0	0	0.5	0.4899	0.4995	97.98	3.11	99.90
Cu ²⁺	0	0	0.5	0.4952	0.5014	99.04	2.05	100.28
Sample 2								
Pb ²⁺	0.5	0.4977	0.5	0.9958	0.9927	99.58	1.22	99.50
Cu ²⁺	0	0.0204	0.5	0.5114	0.5320	102.28	3.17	100.07
Sample 3								
Pb ²⁺	0	0	0.5	0.4985	0.5109	99.70	1.01	102.18
Cu ²⁺	1.5	1.4251	0.5	1.9853	1.9630	99.26	0.85	101.97

The investigation of the selectivity of N-GE modified GCE was conducted with the interferences caused by common metal ion like Co²⁺, Zn²⁺ and Ni²⁺. With the peak current alteration in ±5%, Cu(II) and Pb(II) analysis was not interfered by 50-folds of Co²⁺, Zn²⁺ and Ni²⁺. Thus as-fabricated sensor in this work performs excellently in selectivity and could detect Cu(II) and Pb(II) without being influenced by normal interferences. SWASV eight repetitive stripping voltammograms were employed for the investigation of the stability of the N-GE modified GCE, to detect Cu(II) and Pb(II) (0.5 μM). Relative standard deviations of 1.78% and 2.77% were observed respectively for Cu(II) and Pb(II). To determine Cu(II) and Pb(II) (0.5 μM), the work investigated the reproducibility of the N-GE modified GCE, six freshly prepared electrodes. It could be seen that the sensor was prepared in a process featuring favorable reproducibility, with the relative standard deviation for the peak currents determined as 2.22 %.

4. CONCLUSIONS

This study employed a N-GE modified GCE to detect Cu(II) and Pb(II) simultaneously through a simple and cost-effective electrochemical sensor with great sensitivity, where the preparation was inexpensive and simple preparation. The respective detection limit for Cu(II) and Pb(II) by as-fabricated electrochemical sensor is 5 nM and 11 nM. Herein the linear detection ranges from 0.05 to

2.5 μM . In addition, the proposed electrochemical sensor performed superbly in reproducibility and featured favorable anti-interference trait.

ACKNOWLEDGEMENT

The authors wish to acknowledge the Natural Science Foundation of China (grant numbers 51678552), the Science and Technology Project of Fujian Province (grant numbers 2016Y0082) and the Science and Technology Project of Xiamen (grant numbers 3502Z20162003).

References

1. P. Wongsasuluk, S. Chotpantarat, W. Siriwong and M. Robson, *Environ. Geochem. Health.*, 36 (2014) 169.
2. R. Verma and B. Gupta, *Food Chem.*, 166 (2015) 568.
3. P. Kanagaraj, A. Nagendran, D. Rana, T. Matsuura, S. Neelakandan, T. Karthikkumar and A. Muthumeenal, *Appl. Surf. Sci.*, 329 (2015) 165.
4. X. He, B. Xi, H. Pan, X. Li, D. Li, D. Cui, W. Tang and Y. Yuan, *Environmental Science and Pollution Research*, 21 (2014) 7973.
5. T. Chiroma, R. Ebebele and F. Hymore, *International Refereed Journal of Engineering and Science*, 3 (2014) 01.
6. J. Kpan, B. Opoku and A. Gloria, *Journal of Agricultural Chemistry and Environment*, 3 (2014) 40.
7. D. Setyono and S. Valiyaveetil, *J. Hazard. Mater.*, 302 (2016) 120.
8. X. Peng, G. Shi, G. Liu, J. Xu, Y. Tian, Y. Zhang, Y. Feng and A.G. Russell, *Environ. Pollut.*, 221 (2017) 335.
9. X. Qing, Z. Yutong and L. Shenggao, *Ecotoxicol. Environ. Saf.*, 120 (2015) 377.
10. M. Khan, R. Malik and S. Muhammad, *Chemosphere*, 93 (2013) 2230.
11. F. Zhu, L. Qu, W. Fan, A. Wang, H. Hao, X. Li and S. Yao, *Environmental Monitoring and Assessment*, 187 (2015) 161.
12. M. Wijayawardena, M. Megharaj and R. Naidu, *Advances in Agronomy*, 138 (2016) 175.
13. M. Rajabi, S. Asemipour, B. Barfi, M. Jamali and M. Behzad, *J. Mol. Liq.*, 194 (2014) 166.
14. Y. Unsal, M. Soylak, M. Tuzen and B. Hazer, *Anal. Lett.*, 48 (2015) 1163.
15. A. Safavi, N. Maleki, S. Alizadeh and F. Farjami, *Sensor Letters*, 14 (2016) 769.
16. Z. Al Othman, Y.E. Unsal, M. Habila, A. Shabaka, M. Tuzen and M. Soylak, *Anal. Lett.*, 48 (2015) 1738.
17. J. Ayala-Cabrera, M. Trujillo-Rodríguez, V. Pino, Ó. Hernández-Torres, A. Afonso and J. Sirieix-Plénet, *Int. J. Environ. Anal. Chem.*, 96 (2016) 101.
18. J. Zou, X. Ma, Y. Dang and Y. Chen, *J. Anal. At. Spectrom.*, 29 (2014) 1692.
19. S. Arain, T. Kazi, H. Afridi, A. Abbasi, A. Panhwar, B. Shanker and M. Arain, *Spectrochim. Acta, Part A* 133 (2014) 651.
20. S. de Oliveira Souza, L.L. François, A.R. Borges, M.G.R. Vale and R.G.O. Araujo, *Spectrochim. Acta, Part B*. 114 (2015) 58.
21. L. Cui, J. Wu and H. Ju, *Biosens. Bioelectron.*, 63 (2015) 276.
22. C. Wang, J. Du, H. Wang, C.e. Zou, F. Jiang, P. Yang and Y. Du, *Sens. Actuators, B*, 204 (2014) 302.
23. H. Bagheri, A. Hajian, M. Rezaei and A. Shirzadmehr, *J. Hazard. Mater.*, 324 (2017) 762.
24. K. Novoselov, A. Geim, S. Morozov, D. Jiang, Y. Zhang, S. Dubonos, I. Grigorieva and A. Firsov, *Science*, 306 (2004) 666.
25. J. Li, Z. Xu, M. Liu, P. Deng, S. Tang, J. Jiang, H. Feng, D. Qian and L. He, *Biosens. Bioelectron.*, 90 (2017) 210.

26. B. Huang, L. Xiao, H. Dong, X. Zhang, W. Gan, S. Mahboob, K. Al-Ghanim, Q. Yuan and Y. Li, *Talanta*, (2016)
27. E. Asadian, S. Shahrokhian, A.I. Zad and F. Ghorbani-Bidkorbek, *Sens. Actuators, B.*, 239 (2017) 617.
28. H. Liu, Y. Liu and D. Zhu, *J. Mater. Chem.*, 21 (2011) 3335.
29. S. Lee, R. Belosludov, H. Mizuseki and Y. Kawazoe, *Small*, 5 (2009) 1769.
30. A. Lherbier, X. Blase, Y.-M. Niquet, F. Triozon and S. Roche, *Phys. Rev. Lett.*, 101 (2008) 036808.
31. L. Qu, Y. Liu, J.-B. Baek and L. Dai, *ACS Nano*, 4 (2010) 1321.
32. Z. Sheng, L. Shao, J. Chen, W. Bao, F. Wang and X. Xia, *ACS Nano*, 5 (2011) 4350.
33. X. Wang, X. Li, L. Zhang, Y. Yoon, P.K. Weber, H. Wang, J. Guo and H. Dai, *Science*, 324 (2009) 768.
34. D. Long, W. Li, L. Ling, J. Miyawaki, I. Mochida and S.-H. Yoon, *Langmuir*, 26 (2010) 16096.
35. L. Sun, L. Wang, C. Tian, T. Tan, Y. Xie, K. Shi, M. Li and H. Fu, *Rsc Advances*, 2 (2012) 4498.
36. H. Wang, Q. Hao, X. Yang, L. Lu and X. Wang, *ACS Appl. Mater. Interfaces*, 2 (2010) 821.
37. Z. Lei, L. Lu and X. Zhao, *Environ. Sci. Technol.*, 5 (2012) 6391.
38. Y. Guo, Y. Chen, Q. Zhao, S. Shuang and C. Dong, *Electroanalysis*, 23 (2011) 2400.
39. S. Yang, X. Song, P. Zhang and L. Gao, *ACS Appl. Mater. Interfaces.*, 5 (2013) 3317.
40. D. Jiang, Q. Liu, K. Wang, J. Qian, X. Dong, Z. Yang, X. Du and B. Qiu, *Biosens. Bioelectron.*, 54 (2014) 273.
41. G. Buica, E. Ungureanu, L. Birzan, A. Razus and L. Mandoc, *J. Electroanal. Chem.*, 693 (2013) 67.
42. I. Cesarino, E. Cavalheiro and C. Brett, *Electroanalysis*, 22 (2010) 61.
43. L. Zhu, L. Xu, B. Huang, N. Jia, L. Tan and S. Yao, *Electrochim. Acta* 115 (2014) 471.
44. P. Sahoo, B. Panigrahy, S. Sahoo, A. Satpati, D. Li and D. Bahadur, *Biosens. Bioelectron.*, 43 (2013) 293.
45. H. Lin, M. Li and D. Mihailovič, *Electrochim. Acta*, 154 (2015) 184.